Cellular/Molecular

The Rod Photoreceptor Pattern Is Set at the Optic Vesicle Stage and Requires Spatially Restricted *cVax* Expression

Dorothea Schulte,[1,2] Maureen A. Peters,[1] Jonaki Sen,[1] and Constance L. Cepko[1]

[1]Department of Genetics and Howard Hughes Medical Institute, Harvard Medical School, Boston, Massachusetts 02115, and [2]Max-Planck-Institut für Hirnforschung, 60528 Frankfurt/Main, Germany

How and when positional identities in the neural retina are established have been addressed primarily with respect to the topographic projections of retinal ganglion cells onto their targets in the brain. Although retinotectal map formation is a prominent manifestation of retinal patterning, it is not the only one. Photoreceptor subtypes are arranged in distinct, species-specific patterns. The mechanisms used to establish photoreceptor patterns have been relatively unexplored at the mechanistic level. We performed ablations of the eye anlage in chickens and found that removal of the anterior or dorsal optic vesicle caused loss of the area centralis, which is a rod-free central area of the retina, and severely disorganized other aspects of the rod pattern. These observations indicate that the anteroposterior and dorsoventral distribution of rods is determined by the optic vesicle stage. To investigate the molecular mechanisms involved, the rod distribution was analyzed after viral misexpression of several patterning genes that were previously shown to be important in positional specification of retinal ganglion cells. Ectopic expression of *FoxG1*, *SOHo1*, or *GH6* transcription factors expressed in the anterior optic vesicle and/or optic cup, respectively, did not affect the rod pattern. This pattern therefore appears to be specified by an activity acting before, or in parallel with, these factors. In contrast, misexpression of the ventrally restricted transcription factor, *cVax*, severely disturbed the rod pattern.

Key words: **retina; patterning; photoreceptor; ganglion cell; Vax; development**

Introduction

The faithful representation of visual space begins with the photoreceptor cells. These highly specialized primary sensory neurons are stimulated by light, which triggers a signal transduction cascade. The first step in transforming this information into signals interpretable by the visual centers in the brain begins at the first synapse between photoreceptor cells and bipolar cells. The transformations continue within a second synaptic layer, in which the processed information is transmitted to the retinal ganglion cells (RGCs). RGC projections are topographically precise, indicating that RGCs and their target cells need to posses positional information. The time when this positional information is acquired during development, as well as the mechanisms used by RGCs to find their targets in the brain, have been the subjects of extensive investigations (McLaughlin et al., 2003). Surgical manipulations of the eye anlage demonstrated that cells in the optic vesicle have already acquired positional specification along the anteroposterior (AP) axis, which, when perturbed, alters the mapping behavior of RGCs (Dütting and Thanos, 1995). Recently, several transcription factors have been discovered to have expression domains that subdivide the eye anlage into distinct domains before the production of postmitotic neurons. The anterior expression of the transcription factor *FoxG1* (*BF-1*) and the posterior expression of *FoxD1* (*BF-2*) were observed quite early in the optic vesicle. This was followed slightly later by expression of the homeodomain protein *mHmx1/cGH6* and the related protein *SOHo-1* in the anterior optic cup of chick and medaka (Deitcher et al., 1994; Hatini et al., 1994; Stadler and Solursh, 1994; Adamska et al., 2001). Expression of the homeodomain protein *cVax*/*mVax2* is observed in the ventral optic vesicle, whereas members of the T-box family of transcription factors can be observed in the dorsal optic vesicle (Gibson-Brown et al., 1998; Barbieri et al., 1999; Ohsaki et al., 1999). As shown by gain-of-function and loss-of-function studies, these molecules determine positional specification of RGCs and consequently control the expression of axon guidance cues and the formation of the retinotectal map (Yuasa et al., 1996; Schulte et al., 1999; Koshiba-Takeuchi et al., 2000; Schulte and Cepko, 2000; Barbieri et al., 2002; Mui et al., 2002; Takahashi et al., 2003).

To date, almost every study of the establishment of retinal pattern has used the formation of the retinotectal map as a functional read-out of pattern. However, other cell types are topographically organized within the retina (Masland and Raviola, 2000). Photoreceptor subtypes are usually differentially distributed across the vertebrate retina (for review, see Cepko, 1996).

Received May 26, 2004; revised Jan. 24, 2005; accepted Jan. 25, 2005.

This work was supported by the Howard Hughes Medical Institute, a Human Frontier Science Program fellowship to D.S., and a National Eye Institute training grant to M.A.P. We thank Masaharu Noda for CBF1 (FoxG1)-RCAS(B), Malcolm Logan for TbxEnR-RCAS(A), John Flanagan and Elena Pasquale for probes, Christa Ziegler for excellent technical assistance, and Keely Bumsted–O'Brien and Leo Peichl for helpful comments on this manuscript.

Correspondence should be addressed to either of the following: Constance L. Cepko, Department of Genetics, Harvard Medical School, 77 Avenue Louis Pasteur, Boston, MA 02115, E-mail: cepko@genetics.med.harvard.edu; or Dorothea Schulte, Max-Planck-Institut für Hirnforschung, Deutschordenstrasse 46, 60528 Frankfurt/Main, Germany, E-mail: schulte@mpih-frankfurt.mpg.de.

M. A. Peters's present address: Department of Biology, University of Utah, Salt Lake City, UT 84112.

DOI:10.1523/JNEUROSCI.2037-04.2005

 0270-6474/05/252823-09$15.00/0

The best known example for such a photoreceptor pattern is the human fovea (Curcio et al., 1990, 1991). This specialized area is located approximately in the center of the retina and exhibits a total lack of rods and blue cones. The fovea-specific photoreceptor distribution, together with its circuitry and structure, enable high-acuity color vision under daylight conditions. Despite the obvious importance of this structure, the mechanisms that initiate foveation or specify its location are completely unexplored. Unlike most other vertebrate model organisms, the chick retina contains a central rod-free area (Bruhn and Cepko, 1996). We exploited this aspect of the chick retina to investigate the mechanisms controlling the development of the rod-free area (area centralis). Partial ablations of the eye anlage were performed to determine when the rod pattern was established, and retroviral vectors were used to deliver genes thought to be involved in the development of pattern in the chick retina.

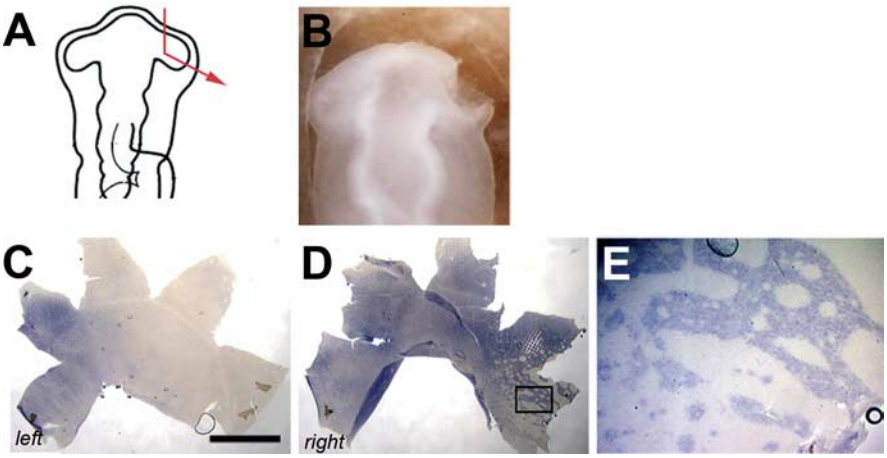

Figure 1. EphA3 expression profile after partial resection of the anterior optic vesicle. ***A***, Schematic of the performed surgery. ***B***, The actual ablation of the specimen. Most of the right anterior optic vesicle was removed *in ovo* at HH stage 11. ***C***, ***D***, Expression of *EphA3*, as visualized by *in situ* hybridization, in the control (***C***, left) and operated (***D***, right) retinas at E7 of the specimen shown in ***B***. (The image of the left retina was mirrored so that, in all panels, dorsal is to the top, ventral is to the bottom, nasal/anterior is to the right, and temporal/posterior is to the left.) Scale bar, 1.5 mm. ***E***, Higher magnification of the boxed area in ***D***, demonstrating clusters of *EphA3*-expressing and -nonexpressing cells.

Materials and Methods

RNA in situ *hybridization.* The probes for *rhodopsin* and *red-* and *green-cone opsin* were described previously (Bruhn and Cepko, 1996). The cDNA clones used to generate *in situ* probes for *EphA3* and *EphB2* were gifts from J. Flanagan (Harvard Medical School, Boston, MA) and E. Pasquale (Burnham Institute, La Jolla, CA), respectively (Cheng et al., 1995; Holash and Pasquale, 1995). *In situ* hybridizations were performed as described previously (Bruhn and Cepko, 1996; Schulte and Cepko, 2000). Because the retinas had to be immobilized between nylon meshes, the mesh pattern occasionally imprinted onto the tissue (see Fig. 2*G*), which was unrelated to the hybridization signal. For higher-magnification images, the retinas were cleared through an ascending series of graded glycerol in PBS and mounted photoreceptor-side up in 100% glycerol.

Partial ablation of the eye anlage. Fertilized White Leghorn eggs (Charles River, Sulzfeld, Germany) were incubated at 38°C for 36–40 h until Hamburger Hamilton (HH) stage 10–11 [10–13 somites; embryonic day 1.5 (E1.5)] and windowed (Hamburger and Hamilton, 1992). For ablation of the eye anlage, the embryo was visualized by injection of a small amount of Higgins fountain pen ink (10% in avian Ringer's solution: 0.85% NaCl, 0.042% KCl, and 0.025% $CaCl_2$) underneath. Various amounts of the right optic vesicle were removed manually with sharpened tungsten needles. After the manipulation, each embryo was photographed with a Nikon (Tokyo, Japan) N6006 camera attached to the dissecting microscope to document the degree and quality of the individual surgery. The eggs were sealed with plastic tape and incubated at 38°C for the times indicated. At E7 (HH stage 31) or E18 (HH stage 44), the embryos were decapitated, and the retinas of control and experimental eyes were collected.

Retroviral misexpression. Replication-competent avian retroviral vectors with a B envelope RCASBP(B) (Hughes et al., 1987) were used for transduction of patterning genes. The RCASBP(B) constructs for RCAS-*SOHo1*, RCAS-*GH6*, and RCAS-*cVax* were described by Schulte and Cepko (2000) and Schulte et al. (1999), respectively. RCASBP(B)-*CBF1* (*FoxG*1) was described by Yuasa et al. (1996) and kindly provided by M. Noda (National Institute for Basic Biology, Okazaki, Japan). RCASBP(A)-*Tbx5EnR* was described by Rallis et al. (2003) and kindly provided by M. Logan (National Institute for Medical Research, Mill Hill, UK). Retroviral stocks were generated as described previously (Schulte and Cepko, 2000). All viral titers were between 1×10^8 and 8×10^8. Polybrene was added to a final concentration of 8 μg/ml, and viral stocks were injected into both optic vesicles at HH stage 10 to HH stage 11 (E1.5).

Results

To test whether the AP and dorsoventral (DV) patterns of the optic vesicle are imparted not only to RGCs for the establishment of retinotopic order but also to cells that establish the rod photoreceptor pattern, ablations were performed essentially as described by Dütting and Thanos (1995). Instead of axon tracing and analysis of the retinotectal map, however, the right experimental and the left control retinas were processed for *in situ* hybridization. Probes for *rhodopsin*, a rod marker, and several genes involved in early patterning were used.

Expression of *EphA3* after removal of the anterior optic vesicle

Eph receptor tyrosine kinases and their membrane-bound ligands, the ephrins, play central roles in the formation of the retinotectal/retinocollicular map, the ordered projections of RGCs to the first visual centers in the brain. *EphA3* in the chick, or its functional ortholog *EphA5* in the mouse, is expressed in a steep gradient on RGCs of the developing retina, high on the posterior (temporal) side and low on the anterior (nasal) side (Fig. 1*A*) (Cheng et al., 1995; Feldheim et al., 1998). Gain-of-function or loss-of-function experiments of these EphA receptors or their ephrins disturbed map development, demonstrating that graded expression of EphA3 or EphA5, respectively, are required for RGC axon guidance and topographic map formation (Nakamoto et al., 1996; Frisén et al., 1998; Hornberger et al., 1999; Brown et al., 2000; Feldheim et al., 2000).

The ablation experiments of Dütting and Thanos were performed before the discovery of the Eph receptors and ephrins (Dütting and Thanos, 1995). Thus, they did not analyze the consequence of their ablations with respect to changes in the expression pattern of these molecules. To explore this and to obtain a suitable standard for the general quality of our surgeries, retinas were processed for *EphA3 in situ* hybridization after partial removal of the anterior optic vesicle. Increasing portions of the right anterior optic vesicle were removed at HH stage 11 (i.e., the tissue normally destined to form the nasal retina and RGCs that

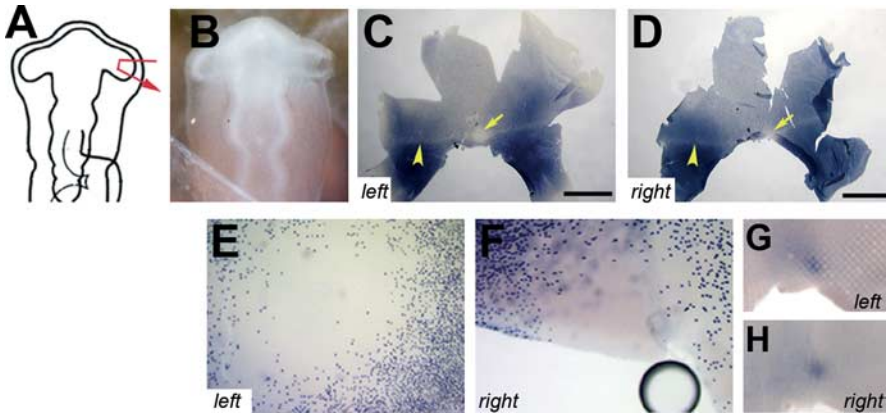

Figure 2. Development of photoreceptor pattern after removal of the distal tip of the optic vesicle. A pie fragment of the right optic vesicle was removed at its distal tip (***A***, ***B***). The distribution of rods at E18 of this embryo is shown after *in situ* hybridization with a *rhodopsin* probe. ***C***, Left, Control retina. ***D***, Right, Operated retina. The arrows in ***C*** and ***D*** indicate the central rod-free zone, and the arrowheads indicate the horizontal rod-sparse streak. ***E***, ***F***, Higher magnification of the area centralis of the above retinas of the left (***E***) and right eye (***F***). ***G***, ***H***, Onset of expression of *red cone opsin* in the control (***G***, left) and experimental (***H***, right) retinas at E14 in another specimen, in which the same surgery was performed. (The images of the left retinas were mirrored so that, in all panels, dorsal is to the top, ventral is to the bottom, nasal/anterior is to the right, and temporal/posterior is to the left.) Scale bars, 3.75 mm.

do not express *EphA3*) (Fig. 1*A*,*B*) ($n = 8$). The embryos were allowed to survive to E7. In five operated retinas (right eyes), the domain of *EphA3* expression extended significantly further into the nasal hemisphere than in the control (left) eyes (Fig. 1*C*,*D*). The extent to which the *EphA3* domain shifted depended on the amount of tissue removed. Figure 1*D* shows the typical outcome of a surgery, in which approximately two-thirds of the anterior vesicle was ablated; the domain of high *EphA3* expression was expanded across the entire retina reaching the nasal periphery, where clusters of *EphA3*-expressing cells and cells not expressing *EphA3* were intermingled (higher magnification is shown in Fig. 1*E*), reminiscent of the mosaic retina described by Thanos et al. (1996). Sharp boundaries formed between the domains of high-level *EphA3* expression and patches of cells lacking *EphA3* expression. The opposite results were obtained when the ablation was done on the posterior optic vesicle (data not shown).

Distribution of rod photoreceptors

Photoreceptor subtypes in almost all vertebrates are distributed in topographically distinct, species-specific patterns. These patterns provide a remarkable adaptation to the life style of the species and must be precisely controlled during development. In the chick retina, rods are arranged in a distinct pattern that is asymmetric along both the AP and DV axes (Fig. 2*C*). There is a prominent gradient of rod density along the DV axis, with rods being more abundant in the ventral than dorsal retina. In addition, the rod-dense area extends dorsally over the horizontal meridian and takes on approximately the shape of a crescent. This crescent itself is asymmetric, because it extends on the anterior side further into dorsal territory than on the posterior side. Moreover, a circular rod-free zone is located approximately in the center of the retina, just anterior of the optic nerve head (Fig. 2*C*, arrow). The rod-free zone is flanked by a narrow band of lower rod density, the rod-sparse streak (Fig. 2*C*, arrowhead), running along the horizontal meridian. The approximate location of the rod-free spot corresponds to the area of highest RGC and amacrine cell density and presumably allows for higher visual acuity in this part of the visual field (Morris, 1982; Straznicky and Chehade, 1987; Bruhn and Cepko, 1996). This area is also the location of the onset of expression of the long and middle wavelength-sensitive cone opsins, similar to the human retina (Bruhn and Cepko, 1996; Xiao and Hendrickson, 2000). Therefore, the chick rod-free zone shares several important features of the primate fovea: its location in the central retina, the absence of rods, and the onset of the expression of long and middle wavelength-sensitive cone opsins (Curcio et al., 1990, 1991; Bruhn and Cepko, 1996).

Specification of the rod-free zone

Cells of the central-most region of the eye anlage comprise the distal tip of the optic vesicle that comes into close contact with the surface ectoderm before optic cup invagination. These cells give rise to the central neural retina, including the rod-free zone (Dütting and Thanos, 1995). A pie slice-shaped portion of the right optic vesicle, together with the overlying surface ectoderm, was ablated at HH stage 10 to determine whether the rod-free zone could develop only from this domain (Fig. 2*A*,*B*). At E18, both left and right retinas were collected, and the distribution of rods was visualized by *in situ* hybridization with a probe specific for *rhodopsin*. In all specimens examined ($n = 9$), the rod pattern in the operated retina was normal (Fig. 2*C*–*F*). In parallel experiments, the onset of long wavelength-sensitive cone opsin expression was monitored at E14 after the same surgery (Fig. 2*G*,*H*). Again, *opsin* expression started in the experimental and control retina in a

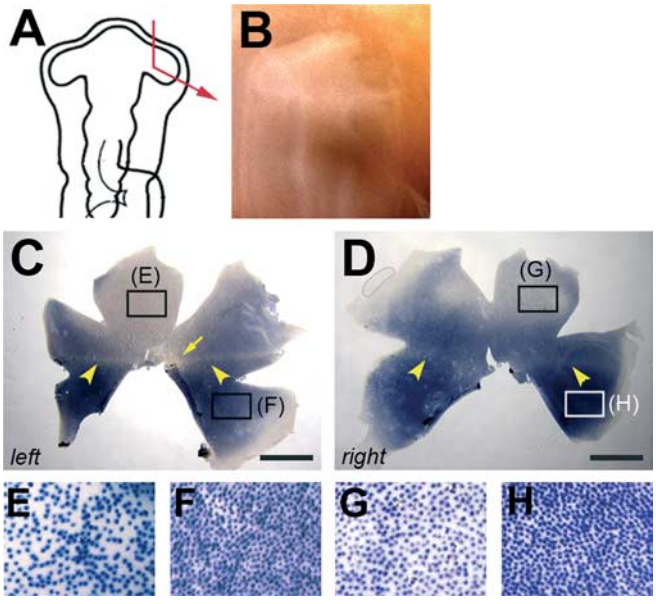

Figure 3. Distribution of rod photoreceptors after ablation of the anterior optic vesicle. Most of the anterior optic vesicle was removed at HH stage 11 (***A***, ***B***). The rod distribution was severely altered in the operated retina (***D***, right) when compared with the control (***C***). The density of rods in the dorsal and ventral areas of both retinas are shown below at higher magnification (***E–H***). The regions from which the pictures were taken are marked by boxes: ***E***, ***F***, higher magnification of the control and left retina on the dorsal (***E***) and ventral (***F***) sides; ***G***, ***H***, higher magnification of the operated right retina dorsally (***G***) and ventrally (***H***). (The image of the left retina was flipped so that, in all panels, dorsal is to the top, ventral is to the bottom, nasal/anterior is to the right, and temporal/posterior is to the left.) Scale bars, 3 mm.

discrete spot located in the central retina ($n = 6$). The place and time of onset of expression were indistinguishable between right and left eyes. The rod-free zone thus can be reconstituted from surrounding tissue after removal of the distal tip.

Distribution of rod photoreceptors after removal of the anterior optic vesicle

Increasing portions of the right anterior optic vesicle were removed at HH stage 10, and the tissue was monitored for the rod photoreceptor pattern at E18 (Fig. 3*A*,*B*) ($n = 12$). Again, as noted for the expression profile of *EphA3* after partial ablation of the vesicle, the degree of disturbance of the rod photoreceptor pattern correlated well with the amount of tissue removed. After removal of 50% of the vesicle or more, the rod pattern was markedly and reproducibly perturbed. Figure 3, *C* and *D*, shows a typical outcome of a surgery, in which two-thirds of the anterior vesicle was removed. First, the rod-sparser dorsal region was reduced in size, whereas the rod-richer, ventral region was expanded. Second, the rod-free zone was missing. Interestingly, the horizontal rod-sparse streak was still visible (Fig. 3*C*,*D*, arrowheads). Figure 3, *E–H*, shows a comparison of areas within the dorsal and ventral regions in the experimental and control retinas at higher magnifications. Rods are relatively evenly spaced in dorsal and ventral retina under both conditions. These data indicate that when 50% or more of the anterior optic vesicle was removed at HH stage 10–11 (E1.5), the rod photoreceptor pattern was markedly altered.

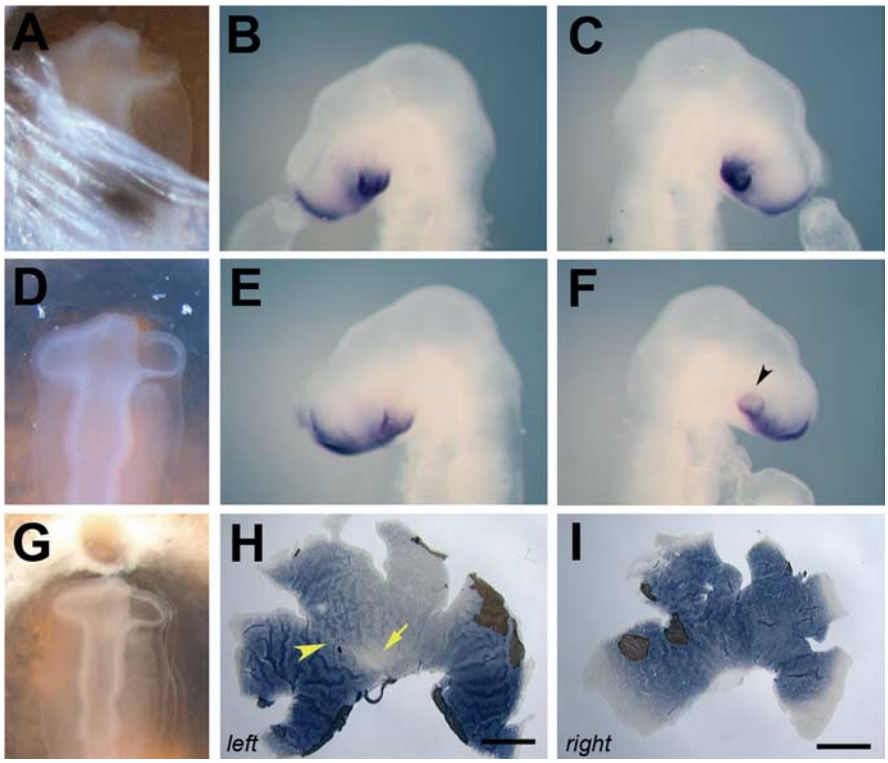

Figure 4. The influence of partial optic vesicle ablation on retinal DV pattern. ***A–C***, *cVax* expression after removal of the anterior eye anlage. The surgery was performed at HH stage 11 (E1.5; ***A***). At HH stage 16 (E2.5), the expression domain of *cVax* was indistinguishable in the left control eye (***B***) and right operated eye (***C***) of the specimen shown in ***A***. ***D–F***, *cVax* expression after removal of the dorsal optic vesicle. The ablation was performed at HH stage 11 (***D***). After 24 h (at HH stage 16), the operated right eye was often smaller in size (***F***) than the left control eye (***E***) and showed ectopic expression of cVax in the dorsal eye cup (***F***, arrowhead). ***G–I***, Distribution of rods after removal of the dorsal eye anlage. Ablation of the dorsal optic vesicle at HH stage 11 (***G***) caused a clear ventralization of the rod pattern at E18 (***H***, ***I***). In the left control retina, the rod-free zone (arrow) and rod-sparse streak (arrowhead) were visible (***H***). In the right operated retina, both structures were missing, and the normal ventral domain of high rod density extended across the entire retina (***I***). In ***H*** and ***I***, remnants of the pigment epithelium still attached to the neural retina are visible. (The image of the left retina was flipped so that, in ***H*** and ***I***, dorsal is to the top, ventral is to the bottom, nasal is to the right, and temporal is to the left.) Scale bars, 3 mm.

Distribution of rod photoreceptors after removal of the dorsal optic vesicle

The observed change in rod distribution after removal of the anterior optic vesicle always included a shift of the ventral rod-rich territory into the dorsal retina (Fig. 3*D*). To test whether this was attributable to a change in the DV pattern of the optic vesicle, the expression pattern of the ventral transcription factor, *cVax*, was monitored after anterior ablation of the optic vesicle (Fig. 4*A–C*) ($n = 20$). *cVax* expression in the ventral forebrain, optic stalk, and ventral neural retina was observed to be indistinguishable between the operated right eye and the control left eye (Fig. 4*B*,*C*). Therefore, an alternative mechanism appears to account for the observed increased rod density in the dorsal retina after anterior ablation.

To investigate whether polar coordinates are already in place along the DV axis of the optic vesicle, the dorsal vesicle was ablated at HH stage 10–11 (Fig. 4*D–I*) ($n = 18$). Removal of the dorsal eye anlage often resulted in loss of the eye or a severe reduction in the eye size (data not shown). Such severely affected specimens were not included in the analysis. In eyes that developed to near normal size ($n = 7$), *cVax* expression was observed to extend into the dorsal optic cup (Fig. 4*D–F*) ($n = 5$), and the rod pattern appeared ventralized. The rod-free area and the rod-sparse streak were missing, and the rod-rich territory was extended across the entire DV axis of the retina (Fig. 4*G–I*).

Rod distribution after retroviral misexpression of early patterning genes *Ectopic* expression of *FoxG1*, *SOHo1*, and *GH6*

The winged-helix transcription factor *FoxG1* and the related homeodomain proteins, *SOHo1* and *GH6*, are expressed in the anterior eye anlage and contribute to retinotectal map formation (Deitcher et al., 1994; Hatini et al., 1994; Stadler and Solursh, 1994; Yuasa et al., 1996; Schulte and Cepko, 2000). Expression of *FoxG1* precedes that of *SOHo1* and *GH6*. Because all three proteins are expressed by most, if not all, proliferating neuroblasts of the anterior eye anlage, they might be involved in the specification of AP features of the rod pattern. This was tested by viral misexpression of *FoxG1*, *SOHo1*, and *GH6*. Figure 5 shows representative examples of these manipulations. The distribution of rod photoreceptors in retinas in which *FoxG1*, *SOHo1*, or *GH6* was ectopically expressed was indistinguishable from the control retinas infected with an RCAS virus carrying alkaline phosphatase, a neutral gene to control for viral gene expression. The level of infection was scored by several means. First, in each set of injections, some specimens were harvested at E7, the peak period of photoreceptor genesis in the chick (Prada et al., 1991), and the level of viral spread was detected by *in situ* hybridization with a RCAS-specific probe. Generally, full infection was achieved with

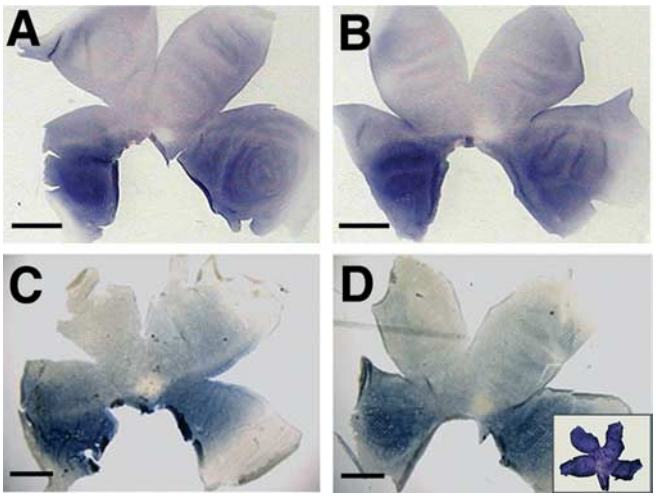

Figure 5. Rod distribution after forced expression of *FoxG1*, *GH6*, and *SOHo1*. ***A–D***, Representative examples of the *rhodopsin* distribution in E18 retinas, in which the expression of the molecules indicated was artificially raised across the entire retina. The rod pattern after retroviral misexpression of *FoxG1* (***B***), *GH6* (***C***), or *SOHo1* (***D***) does not differ from the pattern observed in control retinas, which were infected with a control virus expressing alkaline phosphatase (***A***). In the inset in ***D***, a representative retina infected with RCAS-*SOHo1* was harvested at E7 and stained with a probe specific for the viral *gag* gene, indicating high and uniform infection during the peak period of photoreceptor genesis in the chick. (In all panels, dorsal is to the top, ventral is to the bottom, nasal/anterior is to the right, and temporal/posterior is to the left). Scale bars, 3 mm.

each of the three virus stocks (Fig. 5*D*, inset) (data not shown). Second, because *SOHo1* or *GH6* repress the expression of *EphA3* (Schulte and Cepko, 2000), loss of *EphA3* transcript at E7 served as an additional marker for the activity of the RCAS-*SOHo1* and RCAS-*GH6* viral stocks. This was monitored and consistently observed (data not shown). Infection with RCAS-FoxG1, however, did not alter the expression of EphA3 (data not shown). Moreover, the activity of the viral stocks used was verified by anterograde axon labeling with the fluorescent tracer DiI, which confirmed the previously published observation that ectopic expression of any of these molecules disturbed retinotectal map development (Yuasa et al., 1996; Schulte and Cepko, 2000) (data not shown). Finally, to ensure that only retinas that were fully infected at E18 were scored, the presence of the virus was visualized by immunostaining with an antibody specific to a viral protein after the detection of the rod pattern (data not shown). These data indicate that the rod pattern was not dramatically altered by the ectopic expression of *FoxG1*, *SOHo1*, or *GH6*. However, a minor perturbation in the distribution of rods would likely not have been detected by our assay. Nevertheless, mechanisms other than *FoxG1*, *SOHo-1*, or *GH6* in the eye anlage appear to specify AP asymmetry of the rod photoreceptor pattern in the chick.

Ectopic expression of *cVax* or a dominant-negative form of *Tbx5*

The *Emx*-related transcription factor, *cVax*, is expressed in the optic stalk and ventral optic vesicle. Ectopic expression of *cVax* in the eye anlage ventralized the expression of many markers of retinal DV asymmetry (Eph receptors and their ephrins) as well as perturbed retinotectal projections (Schulte et al., 1999). To test whether the differential distribution of rods across the retina also required ventrally restricted expression of *cVax*, *cVax* was transduced by RCAS, which led to expression throughout the retina ($n = 12$). As shown in Figure 6, the rod pattern was severely altered by this misexpression. The circular rod-free zone was absent in all retinas analyzed (Fig. 6, compare *A*,*B* with *E*,*F*). In addition, the normal dorsal to ventral gradient in rod density was disturbed (Fig. 6*G*,*H*). After ectopic expression of *cVax*, small patches of high-rod density directly bordered patches of low-rod density. The degree of disturbance varied to some extent but correlated well with the extent of infection (data not shown). Because ectopic expression of *cVax* can cause growth retardation of the retina (D. Schulte, M. A. Peters, and C. L. Cepko, unpublished observations), retinas with mild growth reduction were the only ones scored.

Cone subtypes in the chick retina appear to be distributed uniformly across the retina (Bruhn and Cepko, 1996). It would therefore not be expected that their distribution is controlled by DV patterning genes, but it would be possible that their distribution is affected by the change in rod pattern or a result of nonspecific effects of *cVax* misexpression. The distribution of cones expressing the middle wavelength-sensitive ("green") cone opsin was investigated after *cVax* misexpression. No obvious difference in the distribution of cells expressing *green opsin* were observed under these conditions compared with the control (Fig. 6*I–L*) ($n = 10$). Occasionally, retinas did show mild disturbances of green cone distribution ($n = 3$). These retinas, however, were significantly reduced in size compared with that shown in Fig. 6*K*, suggesting that the patterning defect may have been caused by secondary events. They were therefore not included in the analysis.

The T-box transcription factor *Tbx5* is expressed in the dorsal eyecup in a nonoverlapping pattern with *cVax* and has a dorsalizing effect on many aspects of retinal pattern, including the expression of ephrinB1 and ephrinB2 and the formation of the retinotectal projection (Koshiba-Takeuchi et al., 2000; Peters and Cepko, 2002). Dorsal *Tbx5* expression may therefore be an additional requirement for the normal development of the rod photoreceptor pattern. This was tested by ectopic expression of a dominant-negative form of *Tbx5*, in which the DNA binding domain of the Tbx5 protein was fused to the Engrailed repressor domain of *Drosophila melanogaster* (Rallis et al., 2003). Forced expression of *Tbx5-EnR* disturbed the rod pattern (Fig. 6*M–P*). At higher magnification, irregular spacing of rod photoreceptors in the dorsal and ventral hemispheres was obvious (Fig. 6*N–P*). The overall pattern, however, was significantly less affected than what was observed after ectopic expression of *cVax*. This may be attributable to the fact that other Tbx transcription factors, in addition to *Tbx5*, are expressed in the eye, and their activity may not have been blocked by misexpression of *Tbx5-Enr* (Gibson-Brown et al., 1998; Carson et al., 2000; Sowden et al., 2001). In addition, the RCAS-*Tbx5EnR* virus stock had a lower titer than RCAS-*cVax*, which led to incomplete infection (Fig. 5*M*, inset).

Discussion

During invagination of the optic vesicle, the primary axes of the vesicle are retained, such that the DV and AP axes of the optic vesicle correspond to the DV and nasal-temporal axes of the neural retina, respectively (Dütting and Thanos, 1995). Many neuronal cell types of the retina are topographically organized along these axes. For example, RGCs at different retinal locations express different combinations of axon guidance cues and innervate distinct areas of the first visual centers. In addition, photoreceptor subtypes in many vertebrate species show differences in their relative frequencies across the retina (for review, see Cepko, 1996).

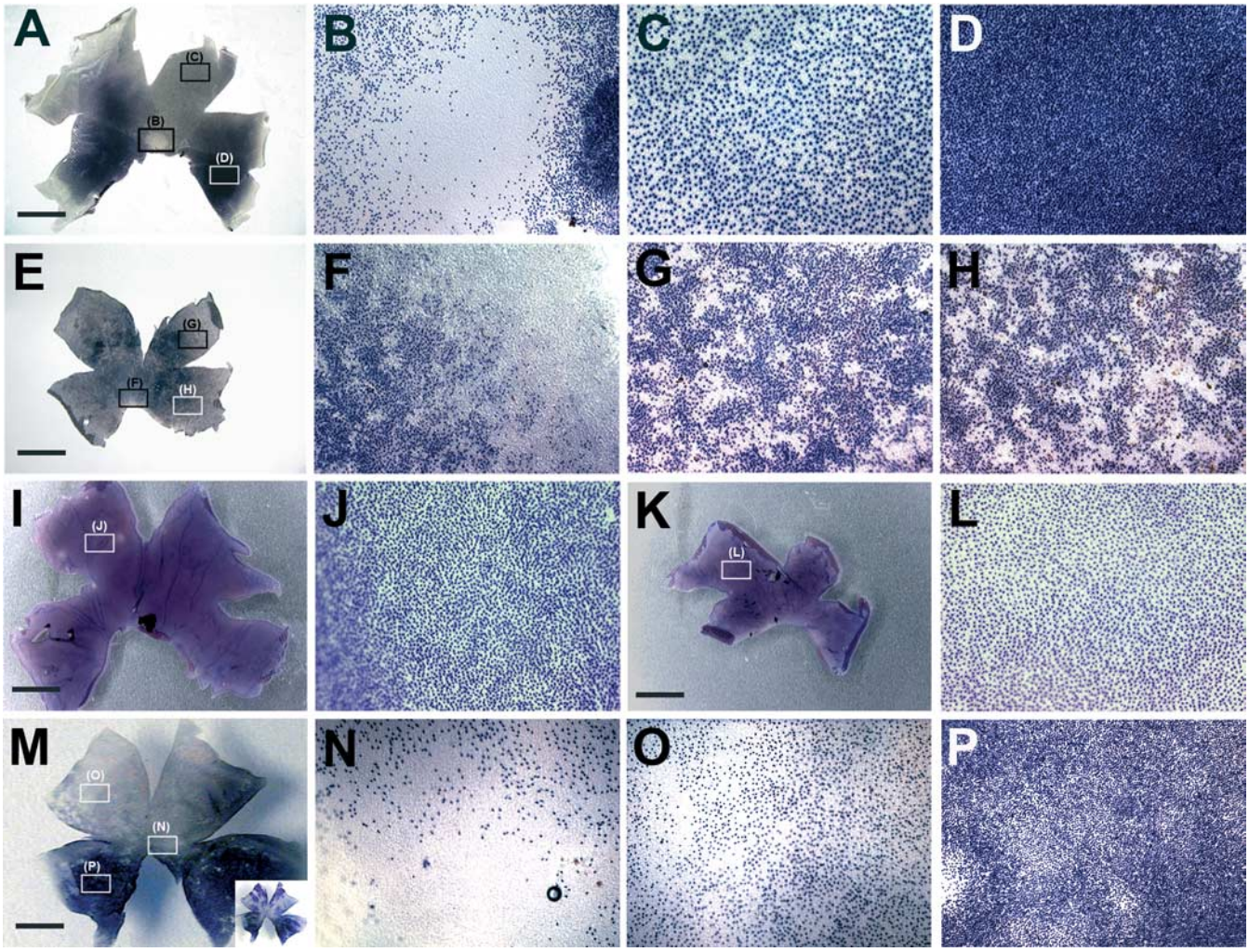

Figure 6. Photoreceptor distribution after forced expression of *cVax* or a putative dominant-negative form of *Tbx5*. ***A***, Distribution and spacing of rods in an uninfected control retina at low magnification. Boxes indicate the regions shown at higher magnification in ***B–D***: the rod-free zone in the central retina (***B***) and dorsal-temporal (***C***) and ventral-temporal (***D***) areas. ***E–H***, Representative results obtained after retroviral misexpression of *cVax*: the rod-free zone did not form, the overall rod distribution was disturbed, and patches of high-rod density were scattered across the retina. ***F–H*** show the randomization of the rod distribution in higher magnification. The regions from which the pictures were taken are indicated by boxes in ***E***. Cones expressing *green opsin* are evenly distributed along AP and DV axes (***I***). Ectopic *cVax* expression under similar conditions as used for ***E–H*** did not affect this pattern (***K***). ***J***, ***L***, Higher-magnification views of two additional examples: green cones of an uninfected control (***J***) and RCAS-cVax infected experimental retina (***L***) were evenly spaced. ***M–P***, Representative results observed after ectopic expression of *Tbx5-EnR*. ***N–P***, High-magnification images of the areas marked by boxes in ***M*** showing irregular spacing of rod photoreceptors. The inset in ***M*** shows the degree of infection with RCAS-Tbx5EnR in the retina depicted in ***M***, visualized by two-color *in situ* hybridization as described by Schulte and Cepko (2000), with detection of the rhodopsin transcripts in dark blue and the viral RNA in pink. (In all panels, dorsal is to the top, ventral is to the bottom, nasal/anterior is to the right, and temporal/posterior is to the left.) Scale bars, 3.75 mm.

Early determination of the AP axis

As shown by surgical manipulations of the eye anlage in different vertebrate species, the retinotopic specificity of RGCs along the retinal AP axis is established at, or before, the formation of the optic vesicles. These identities are therefore established before the generation of postmitotic neurons and their differentiation. Here, the rod photoreceptor distribution of the chick was examined after similar ablations of the optic vesicle. In initial experiments, we asked whether the central eye anlage (i.e., the distal tip of the optic vesicle) was required for the formation of the photoreceptor patterns of the central retina, or area centralis. Removal of the distal tip had no effect on the formation of the rod-free zone or on the timing and location of the onset of red and green cone opsins. These data indicate that the area centralis either is not specified by the optic vesicle stage or that it can be entirely reconstituted by the surrounding tissue (Fig. 2). In contrast, removal of the anterior optic vesicle not only caused a clear shift in the expression domain of *EphA3*, a marker for AP topography of RGCs, but also resulted in significant alterations of the rod distribution across the retina (Figs. 1, 3). Most strikingly, the dorsal rod-sparse region was reduced in size, and the ventral rod-rich area was expanded. Removal of the dorsal optic vesicle led to a similar shift in rod density (Fig. 4). These observations indicate that the AP and DV coordinates that are relevant for the distribution of rods are already assigned by the optic vesicle stage. Figure 7 summarizes the results of these experiments. The rod pattern of the adult retina requires the AP and DV positional identities that are established by the optic vesicle stage, and these identities are stable after surgery (Fig. 7*A*). If the anterior and central optic vesicle is removed, the posterior stump has the capacity to expand across the entire retina (Fig. 7*C*) to generate the rod-sparse horizontal streak, but not the area centralis, or the majority of the dorsal rod-sparse domain (Fig. 7*B*). Likewise, removal of the dorsal and central optic vesicle resulted in a retina reconstituted by proliferation of cells of the ventral optic vesicle (Fig. 7*D*). Consequently, the resulting retina did not contain normal dor-

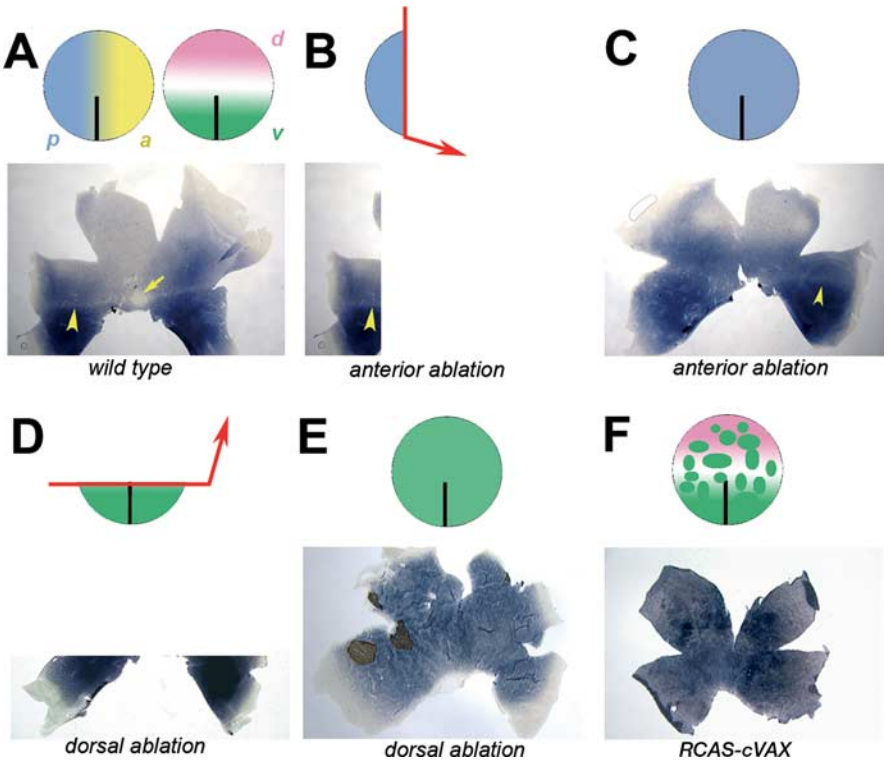

Figure 7. Altered rod distribution after resection of the anterior eye anlage. ***A***, The optic vesicle, schematically represented as circles, is polarized along the AP of the vesicle by several known and unknown factors. Anterior positional values are indicated by a yellow gradient, and posterior values are indicated by a blue gradient. Along the DV axis, the eye anlage is separated into the domains of expression of *cVax* ventrally (green) and *Tbx5* dorsally (pink). Cells along the horizontal meridian of the optic vesicle express neither molecule. The normal rod pattern develops under the influence of these factors. ***B***, Removal of the anterior eye anlage will leave a remnant of the optic vesicle behind of almost maximal posterior characteristics. These cells can only give rise to the posterior-most aspect of the rod pattern. ***C***, When the optic vesicle reconstitutes by proliferation of the remaining cells, the cells appear to retain the positional information they had before the surgery. Consequently, the vesicle remnant gives rise to a retina in which the rod distribution resembles a repetition of the most posterior aspect of the pattern: a dorsal shift of the rod-rich ventral domain containing a rod-sparse streak but no rod-free zone. ***D***, Removal of the dorsal optic vesicle leaves a ventral remnant of the vesicle behind. ***E***, After reconstitution, the healed optic vesicle is entirely composed of cells of ventral origin. Hence, the retina developing from such a vesicle is ventralized with respect to the rod distribution. ***F***, Retroviral misexpression of cVax generates random patches of ectopic *cVax* expression scattered across the optic vesicle and thereby creates numerous new boundaries between cells expressing high levels of *cVax* and cells not expressing *cVax*. This leads to an altered distribution of rods across the retina.

sal or central characteristics, such as the rod-free zone (Fig. 7*E*), rod-sparse horizontal streak, or rod-poor dorsal domain.

Molecular mechanisms specifying rod photoreceptor distribution

The nature and sources of the rod patterning activities are unknown. Positional coordinates may be assigned to the optic vesicle itself, either as a step function (Fig. 7) or in smooth gradients. Proteins asymmetrically expressed along the AP axis of the optic vesicle have been identified by two-dimensional gel electrophoresis (Thanos et al., 1996). They are, however, not yet characterized, and it is unclear whether any contribute to photoreceptor development and/or retinotectal map formation. Alternatively, tissue surrounding the optic vesicle could be the source of the patterning activity, which was removed during the ablation. It has been shown that signals from the surface ectoderm and extraocular mesenchyme partition the optic vesicle into the future domains of neural retina and pigmented epithelium (Pittack et al., 1991, 1997; Hyer et al., 1998; Fuhrmann et al., 2000). It is currently unclear whether these or other signals from surrounding tissue also pattern the prospective neural retina itself. In any respect, retinal progenitor cells must have adopted positional identities by the optic vesicle stage, which are stable and later evident from the mapping behavior of RGCs and the topography of rod photoreceptors.

The transcription factors *FoxG1*, *SOHo1*, and *GH6* are expressed in the anterior eye anlage (Deitcher et al., 1994; Hatini et al., 1994; Stadler and Solursh, 1994). When ectopically expressed, these molecules directly or indirectly repress *EphA3* expression and perturb the proper mapping of some RGCs to the optic tectum (Yuasa et al., 1996; Schulte and Cepko, 2000; Takahashi et al., 2003). All three transcription factors are present on the majority, if not all, retinal progenitor cells within the anterior eye. Yet, they do not appear to contribute in a major way to the specification of anterior retinal characteristics, because their retroviral misexpression had no obvious effect on the overall rod pattern (Fig. 5). Additional mechanisms must therefore exist, which act in parallel with or upstream of these factors. This is in keeping with the observation that the AP axis of the retina is set before expression of *FoxG1*, *SOHo1*, and *GH6*. An initial AP axis of the future retina may be set along with the main body axis, when the eye anlage comprises a region of the neural plate known as the optic pit. It was shown that expression of *FoxG1* in the retina depends on expression of *Pax6*, which led to the conclusion that *Pax6* acts upstream in the control of retinal AP polarity (Bäumer et al., 2002). However, an alternative explanation is that retinal *FoxG1* expression requires the existence of retinal characteristics conveyed by previous expression of *Pax6*, for which expression is critical for normal eye development (Hill et al., 1991; Halder et al., 1995).

In contrast to the AP axis, much progress has been made in elucidating the mechanisms underlying DV axis specification of the neural tube in general and the neural retina in particular. The secreted molecules Sonic Hedgehog and bone morphogenetic protein 4 (BMP4) play central roles in this process (Briscoe and Ericson, 2001; Zhang and Yang, 2001; Peters, 2002; Take-uchi et al., 2003). DV axis specification in the neural retina takes places between HH stages 9 and 12 (Uemonsa et al., 2002). Several retina-specific molecules are expressed during this time in development and have been shown to be involved in this process. They include the transcription factor *cVax/mVax2* and the BMP antagonist *ventroptin* in the ventral eye anlage as well as T-box transcription factors dorsally (Barbieri et al., 1999; Ohsaki et al., 1999; Schulte et al., 1999; Koshiba-Takeuchi et al., 2000; Sakuta et al., 2001; Sowden et al., 2001). The nearly coincident establishment of the DV axis and the appearance of the ventral pattern of expression of cVax might suggest that cVax is higher in the hierarchy of pattern formation than are *FoxG1*, *SOHo1*, and *GH6*, which occur later than AP axis specification. Ectopic expression of *cVax* in the chick embryo or targeted deletion of it in the mouse

did indeed cause major DV pattern abnormalities. There was aberrant expression of many markers of retinal DV asymmetry and severely altered retinotectal projections (Schulte et al., 1999; Barbieri et al., 2002; Mui et al., 2002). As shown here, ectopic *cVax* expression also severely perturbed the rod pattern. Instead of the regular spacing of rods, patches of high-rod density surrounded by areas of low-rod density were found scattered across the RCAS-*cVax*-infected retinas (Fig. 6*E–H*). This phenotype does not resemble the simple ventralization observed after removal of the dorsal optic vesicle (Figs. 4*I*, 7*E*) but, rather, a randomization of the rod pattern. A likely explanation comes from a distinctive feature of retroviral misexpression: during the initial phase of the experiment, cells are infected randomly in the optic vesicle, creating many scattered patches of ectopic *cVax* expression (Fig. 7*F*). Only after further viral spread and division of infected cells will the surrounding tissue begin to ectopically express *cVax* as well. If the rod pattern is initially aligned along *cVax* expressing and *cVax* nonexpressing domains, random ectopic areas of high *cVax* expression should result in random patches of high-rod density. This idea is supported by the observation that ectopic expression of *cVax* caused scattered areas of increased cell density in the photoreceptor layer compared with uninfected control retinas (data not shown).

The ventralizing activity of *cVax* in the retina is juxtaposed by the dorsalizing activity of T-box transcription factors, such as *Tbx5*. Ectopic expression of a dominant-negative form of *Tbx5* also disturbed the rod pattern (Fig. 6*M–P*). *cVax* and *Tbx5* appear to negatively regulate each other's expression (Schulte et al., 1999; Koshiba-Takeuchi et al., 2000). Yet, their expression domains in normal development do not border directly but are separated by a domain that expresses neither molecule (Peters and Cepko, 2002). Diffusible factors must therefore underlie the mutual repression of these two transcription factors. The zone of maximum activity of such diffusible factors would be expected to be the domain that lacks *cVax* and *Tbx5* expression. According to the fate maps of the optic vesicle, the rod-free zone and rod-sparse streak develop in just this domain. The diffusible factors mediating this effect are not known at present but may include retinoic acid (RA), because application of RA in the developing zebrafish resulted in precocious differentiation of rod photoreceptors (Hyatt et al., 1996). In the mouse retina, rods appear to be uniformly distributed across the retina (Jeon et al., 1998), but expression of S- and M-cone opsins differs along the DV axis (Applebury et al., 2000). Although it is still unclear how this pattern is specified, ventrally restricted *mVax2* expression may be necessary for regional differences in cone opsin expression.

References

Adamska M, Wolff A, Kreusler M, Wittbrodt J, Braun T, Bober E (2001) Five Nkx5 genes show differential expression patterns in anlagen of sensory organs in medaka: insight into the evolution of the gene family. Dev Genes Evol 211:338–349.

Applebury ML, Antoch MP, Baxter LC, Chun LL, Falk JD, Farhangfar F, Kage K, Krzystolik MG, Lyass LA, Robbins JT (2000) The murine cone photoreceptor: a single cone type expresses both S and M opsins with retinal spatial patterning. Neuron 27:513–523.

Barbieri AM, Lupo G, Bulfone A, Andreazzoli M, Mariani M, Fougerousse F, Consalez GG, Borsani G, Beckmann JS, Barsacchi G, Ballabio A, Banfi S (1999) A homeobox gene, vax2, controls the patterning of the eye dorsoventral axis. Proc Natl Acad Sci USA 96:10729–10734.

Barbieri AM, Broccoli V, Bovolenta P, Alfano G, Marchitiello A, Mocchetti C, Crippa L, Bulfone A, Marigo V, Ballabio A, Banfi S (2002) Vax2 inactivation in mouse determines alteration of the eye dorsal-ventral axis, misrouting of the optic fibres and eye coloboma. Development 129:805–813.

Bäumer N, Marquardt T, Stoykova A, Ashery-Padan R, Chowdhury K, Gruss P (2002) Pax6 is required for establishing naso-temporal and dorsal characteristics of the optic vesicle. Development 129:4535–4545.

Briscoe J, Ericson J (2001) Specification of neuronal fates in the ventral neural tube. Curr Opin Neurobiol 11:43–49.

Brown A, Yates PA, Burrola P, Ortuno D, Vaidya A, Jessell TM, Pfaff SL, O'Leary DD, Lemke G (2000) Topographic mapping from the retina to the midbrain is controlled by relative but not absolute levels of EphA receptor signaling. Cell 102:77–88.

Bruhn SL, Cepko CL (1996) Development of the pattern of photoreceptors in the chick retina. J Neurosci 16:1430–1439.

Carson CT, Kinzler ER, Parr BA (2000) Tbx12, a novel T-box gene, is expressed during early stages of heart and retinal development. Mech Dev 96:137–140.

Cepko CL (1996) The patterning and onset of opsin expression in vertebrate retinae. Curr Opin Neurobiol 6:542–546.

Cheng HJ, Nakamoto M, Bergemann AD, Flanagan JG (1995) Complementary gradients in expression and binding of ELF-1 and Mek4 in development of the topographic retinotectal projection map. Cell 82:371–381.

Curcio CA, Sloan KR, Kalina RE, Hendrickson AE (1990) Human photoreceptor topography. J Comp Neurol 292:497–523.

Curcio CA, Allen KA, Sloan KR, Lerea CL, Hurley JB, Klock I, Milam AH (1991) Distribution and morphology of human cone photoreceptors stained with anti-blue opsin. J Comp Neurol 312:610–624.

Deitcher DL, Fekete DM, Cepko CL (1994) Asymmetric expression of a novel homeobox gene in vertebrate sensory organs. Neuroscience 14:486–498.

Dütting D, Thanos S (1995) Early determination of nasal-temporal retinotopic specificity in the eye anlage of the chick embryo. Dev Biol 167:263–281.

Feldheim DA, Vanderhaeghen P, Hansen MJ, Frisén J, Lu Q, Barbacid M, Flanagan JG (1998) Topographic guidance labels in a sensory projection to the forebrain. Neuron 21:1303–1313.

Feldheim DA, Kim YI, Bergemann AD, Frisén J, Barbacid M, Flanagan JG (2000) Genetic analysis of ephrin-A2 and ephrin-A5 shows their requirement in multiple aspects of retinocollicular mapping. Neuron 25:563–574.

Frisén J, Yates PA, McLaughlin T, Friedman GC, O'Leary DD, Barbacid M (1998) Ephrin-A5 (AL-1/RAGS) is essential for proper retinal axon guidance and topographic mapping in the mammalian visual system. Neuron 20:235–243.

Fuhrmann S, Levine EM, Reh TA (2000) Extraocular mesenchyme patterns the optic vesicle during early eye development in the embryonic chick. Development 127:4599–4609.

Gibson-Brown JJ, Agulnik I, Silver LM, Papaioannou VE (1998) Expression of T-box genes Tbx2-Tbx5 during chick organogenesis. Mech Dev 74:165–169.

Halder G, Callaerts P, Gehring WJ (1995) Induction of ectopic eyes by targeted expression of the eyeless gene in *Drosophila*. Science 267:1788–1792.

Hamburger V, Hamilton HL (1992) A series of normal stages in the development of the chick embryo. 1951. Dev Dyn 195:231–272.

Hatini V, Tao W, Lai E (1994) Expression of winged helix genes, BF-1 and BF-2, define adjacent domains within the developing forebrain and retina. J Neurobiol 25:1293–1309.

Hill RE, Favor J, Hogan BL, Ton CC, Saunders GF, Hanson IM, Prosser J, Jordan T, Hastie ND, van Heyningen V (1991) Mouse small eye results from mutations in a paired-like homeobox-containing gene. Nature 354:522–525.

Holash JA, Pasquale EB (1995) Polarized expression of the receptor protein tyrosine kinase Cek5 in the developing avian visual system. Dev Biol 172:683–693.

Hornberger MR, Dütting D, Ciossek T, Yamada T, Handwerker C, Lang S, Weth F, Huf J, Wessel R, Logan C, Tanaka H, Drescher U (1999) Modulation of EphA receptor function by coexpressed ephrinA ligands on retinal ganglion cell axons. Neuron 22:731–742.

Hughes SH, Greenhouse JJ, Petropoulos CJ, Sutrave P (1987) Adaptor plasmids simplify insertion of foreign DNA into herpes-independent retroviral vectors. J Virol 61:3004–3012.

Hyatt GA, Schmitt EA, Fadool JM, Dowling JE (1996) Retinoic acid alters photoreceptor development *in vivo*. Proc Natl Acad Sci USA 93:13298–13303.

Hyer J, Mima T, Mikawa T (1998) FGF1 patterns the optic vesicle by directing the placement of the neural retina domain. Development 125:869–877.

Jeon CJ, Strettoi E, Masland RH (1998) The major cell populations of the mouse retina. J Neurosci 18:8936–8946.

Koshiba-Takeuchi K, Takeuchi JK, Matsumoto K, Momose T, Uno K, Hoepker V, Ogura K, Takahashi N, Nakamura H, Yasuda K, Ogura T (2000) Tbx5 and the retinotectum projection. Science 287:134–137.

Masland RH, Raviola E (2000) Confronting complexity: strategies for understanding the microcircuitry of the retina. Annu Rev Neurosci 23:249–284.

McLaughlin T, Hindges R, O'Leary DD (2003) Regulation of axial patterning of the retina and its topographic mapping in the brain. Curr Opin Neurobiol 13:57–69.

Morris VB (1982) An afoveate area centralis in the chick retina. J Comp Neurol 210:198–203.

Mui SH, Hindges R, O'Leary DD, Lemke G, Bertuzzi S (2002) The homeodomain protein Vax2 patterns the dorsoventral and nasotemporal axes of the eye. Development 129:797–804.

Nakamoto M, Cheng HJ, Friedman GC, McLaughlin T, Hansen MJ, Yoon CH, O'Leary DD, Flanagan JG (1996) Topographically specific effects of ELF-1 on retinal axon guidance *in vitro* and retinal axon mapping *in vivo*. Cell 86:755–766.

Ohsaki K, Morimitsu T, Ishida Y, Kominami R, Takahashi N (1999) Expression of the Vax family homeobox genes suggests multiple roles in eye development. Genes Cells 4:267–276.

Peters MA (2002) Patterning the neural retina. Curr Opin Neurobiol 12:43–48.

Peters MA, Cepko CL (2002) The dorsal-ventral axis of the neural retina is divided into multiple domains of restricted gene expression which exhibit features of lineage compartments. Dev Biol 251:59–73.

Pittack C, Jones M, Reh TA (1991) Basic fibroblast growth factor induces retinal pigment epithelium to generate neural retina *in vitro*. Development 113:577–588.

Pittack C, Grunwald GB, Reh TA (1997) Fibroblast growth factors are necessary for neural retina but not pigmented epithelium differentiation in chick embryos. Development 124:805–816.

Prada C, Puga J, Perez-Mendez L, Lopez R, Ramirez G (1991) Spatial and temporal patterns of neurogenesis in the chick retina. Eur J Neurosci 3:559–569.

Rallis C, Bruneau BG, Del Buono J, Seidman CE, Seidman JG, Nissim S, Tabin CJ, Logan MP (2003) Tbx5 is required for forelimb bud formation and continued outgrowth. Development 130:2741–2751.

Sakuta H, Suzuki R, Takahashi H, Kato A, Shintani T, Iemura S, Yamamoto TS, Ueno N, Noda M (2001) Ventroptin: a BMP-4 antagonist expressed in a double-gradient pattern in the retina. Science 293:111–115.

Schulte D, Cepko CL (2000) Two homeobox genes define the domain of EphA3 expression in the developing chick retina. Development 127:5033–5045.

Schulte D, Furukawa T, Peters MA, Kozak CA, Cepko CL (1999) Misexpression of the Emx-related homeobox genes cVax and mVax2 ventralizes the retina and perturbs the retinotectal map. Neuron 24:541–553.

Sowden JC, Holt JK, Meins M, Smith HK, Bhattacharya SS (2001) Expression of *Drosophila* omb-related T-box genes in the developing human and mouse neural retina. Invest Ophthalmol Vis Sci 42:3095–3102.

Stadler HS, Solursh M (1994) Characterization of the homeobox-containing gene GH6 identifies novel regions of homeobox gene expression in the developing chick embryo. Dev Biol 161:251–262.

Straznicky C, Chehade M (1987) The formation of the area centralis of the retinal ganglion cell layer in the chick. Development 100:411–420.

Takahashi H, Shintani T, Sakuta H, Noda M (2003) CBF1 controls the retinotectal topographical map along the anteroposterior axis through multiple mechanisms. Development 130:5203–5215.

Take-uchi M, Clarke JD, Wilson SW (2003) Hedgehog signalling maintains the optic stalk-retinal interface through the regulation of Vax gene activity. Development 130:955–968.

Thanos S, Mey J, Dütting D, Hummler E (1996) Positional determination of the naso-temporal retinal axis coincides with asymmetric expression of proteins along the anterior-posterior axis of the eye primordium. Exp Eye Res 63:479–492.

Uemonsa T, Sakagami K, Yasuda K, Araki M (2002) Development of dorsal-ventral polarity in the optic vesicle and its presumptive role in eye morphogenesis as shown by embryonic transplantation and *in ovo* explant culturing. Dev Biol 248:319–330.

Xiao M, Hendrickson A (2000) Spatial and temporal expression of short, long/medium, or both opsins in human fetal cones. J Comp Neurol 425:545–559.

Yuasa J, Hirano S, Yamagata M, Noda M (1996) Visual projection map specified by topographic expression of transcription factors in the retina. Nature 382:632–635.

Zhang XM, Yang XJ (2001) Temporal and spatial effects of Sonic hedgehog signaling in chick eye morphogenesis. Dev Biol 233:271–290.